Time-domain measurement of intersubband oscillations in a quantum well

James N. Heyman[a)]
Department of Physics and Astronomy, Macalester College, St. Paul, Minnesota 55105

Roland Kersting and Karl Unterrainer
Institut für Festkörperelektronik, TU-Wien, Floragasse 7, A-1040 Wien, Austria

(Received 21 October 1997; accepted for publication 9 December 1997)

We report time-domain measurements of electron intersubband oscillations in quantum wells. We use an interferometric technique to measure the change in the profile of a few-cycle THz pulse due to propagation through a modulation-doped $Al_{0.3}Ga_{0.7}As/GaAs$ multiple quantum well structure (10×510 Å wells). From this data we obtain the absorption and the index of refraction due to electrons in the quantum well, and due to the GaAs substrate. Unlike existing studies of coherent charge oscillations of electrons and holes in heterostructures excited by ultrashort pulses of band-gap light, our all-THz measurements quantitatively determine the linear optical properties of the quantum well electrons. [S0003-6951(98)02306-7]

In time-domain spectroscopy the time evolution of a system is measured following impulsive excitation. The ability to generate ultrashort pulses of terahertz (THz) radiation has made time-domain spectroscopy possible at THz frequencies (THz–TDS).[1] THz-TDS has emerged as an important technique for studying carrier dynamics in quantum wells (QWs), in which carriers scatter and dephase on picosecond time scales. We are interested in understanding carrier scattering and dephasing in quantum wells because these processes are important for the design THz sources and detectors based on intersubband transitions.

Several authors have investigated coherent charge oscillations in quantum wells following pulsed interband excitation. Roskos *et al.*[2] used ultrashort laser pulses to excite a coupled double quantum well, producing excitons in a coherent superposition of states. They observed THz emission due to the resulting coherent tunneling of electrons between the two wells. Planken *et al.*[3] observed THz emission from a single quantum well by coherent excitation of holes into the light and heavy hole subbands. THz emission due to transient Bloch oscillations in a superlattice was reported by Waschke *et al.*[4] Bonvalet *et al.*[5] have used the THz emission to determine both the dephasing rate and the lifetime of excitons in a single quantum well. Sequences of ultrashort laser pulses have also been used to coherently control exciton populations. Brener *et al.*[6] have studied coherent terahertz radiation from quantum wells when the exciting optical fields were shaped both in amplitude and phase. Heberle *et al.*[7] used a sequence of phase-locked femtosecond pulses to create and destroy a charge oscillation in a quantum well, demonstrating that optical nonlinearities can be switched on and off in a time shorter than the phase relaxation time.

Few-cycle THz radiation can be used to perform linear optical spectroscopy in the time domain. This technique can be applied to free carriers and carriers in quantum wells. Some and Nurmikko[8] have used few-cycle THz radiation to detect coherent cyclotron resonance oscillations by free electrons in modulation-doped heterostructures. In this letter, we present the first linear spectra of intersubband transitions of electrons in quantum wells measured by THz-time domain spectroscopy. Unlike frequency domain or Fourier transform spectroscopy, THz-TDS can be combined with pulsed excitation to perform time-resolved spectroscopy on picosecond time scales. Additionally, the technique we present here allows simultaneous measurement of both absorption and dispersion.

In our time-resolved experiments, 80 fs pulses from a Tsunami Ti-sapphire laser are divided at a beamsplitter into *sample* and *analysis* beams (see inset, Fig. 1). The *sample* beam is used to generate few-cycle THz pulses by exciting coherent plasma oscillations in $n=10^{17}$ cm^{-3} doped bulk GaAs.[9] The energy in each THz pulse is of the order 10^{-16} J

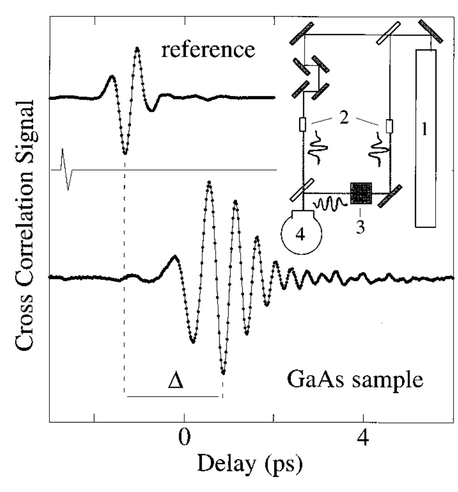

FIG. 1. Cross-correlation signal (dots) measured with no sample (above) and with the 6.06 mm long edge-coupled quantum well sample ($T=6$ K) (below). The solid lines are guides to the eye. In this measurement the quantum wells are depleted of charge. The change in the cross-correlation signal is due to the frequency-dependent index of refraction of the semi-insulating GaAs substrate. The time offset between the signals is $\Delta=52.2$ ps. (Inset) Schematic diagram of experimental apparatus. An 80 fs $\lambda=800$ nm Ti-sapphire laser (1) produces few-cycle THz pulses at the emitters (2). THz pulses are transmitted through the sample (3) and mixed with reference THz pulses at a beamsplitter. We detect the superposition of the pulses as a function of the delay between them with a bolometer (4).

a)Electronic mail: heyman@macalester.edu

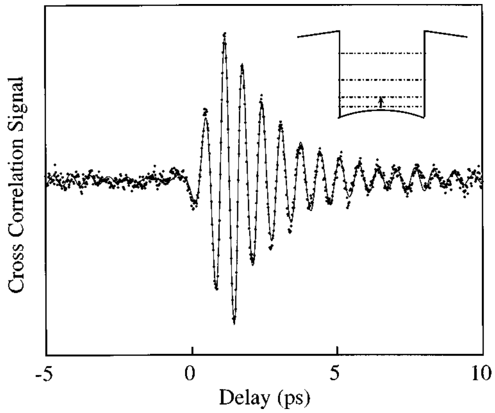

FIG. 2. Measured cross-correlation signal (dots) obtained by modulating the charge density in the 510 Å quantum well sample, and recording the change in transmission with a lock-in amplifier. The THz pulse excites electrons into a coherent superposition of states in the lowest two subbands (see sketch in inset). The solid line is a simulation calculated from a single-oscillator model of the quantum well response and the reference cross-correlation signal.

($\sim 10^5$ photons). This THz radiation is transmitted through the sample. The *analysis* beam is sent through a variable delay stage, and is then used to generate approximately single-half-cycle THz pulses at a low temperature (LT) GaAs epitaxial layer on semi-insulating (SI)-GaAs. Time resolution is obtained by mixing the sample and analysis THz pulses at a Ge beamsplitter and detecting the superposition with an integrating detector (4.2 K Si bolometer) as a function of the delay between pulses. To enhance the signal-to-noise ratio in these cross-correlation measurements, the sample and analysis beams are modulated at separate frequencies and the signal is detected in double modulation using two lock-in amplifiers.

The design of our modulation-doped multiple quantum well structure consists of ten periods of symmetrically modulation doped 510 Å GaAs wells separated by 1600 Å $Al_{0.3}Ga_{0.7}As$ buffers, grown on a SI GaAs substrate. The sample has an aluminum Schottky gate on the surface and AuGe alloyed ohmic contacts on the quantum wells. The wells can be depleted of carriers by applying a negative gate voltage to the Schottky gate, and the zero-bias carrier density in each well was measured to be $n_s = 2.75 \times 10^{10}$ cm^{-2} by capacitance–voltage techniques. For THz measurements, the sample was mounted in an optical cryostat and cooled to 6 K. The THz pulses are coupled into the cleaved edge of the quantum well sample with electric field **E** parallel to the growth direction to excite the intersubband transition.

We recorded the cross-correlation signal under four conditions: (1) with no sample, (2) with the sample fully depleted (-10 V gate bias), (3) with the sample at 0 V bias, and (4) with the gate bias modulated between 0 and -10 V. The first measurement is a reference, while the second probes the optical properties of the depleted sample. After propagation through the depleted sample (see Fig. 1) the THz pulse is delayed and dramatically chirped: the high-frequency components are delayed relative to the low-frequency components. As discussed below, this is due to the frequency-dependent index of refraction of the SI-GaAs substrate.

Figure 2 shows the differential cross-correlation signal measured by modulating the QW carrier density between $n_s = 2.75 \times 10^{10}$ cm^{-2} and depleted. The signal contains only a narrow band of frequency components, and so is not distorted much by the chirp. It arises because the incident THz pulse excites carriers into a coherent superposition of states in the first and second subbands. The resulting coherent charge oscillation radiates along the propagation direction of the incident beam. The signal from the carriers rises during the first 2 ps in response to the THz field. The carriers continue to radiate after the driving THz pulse is over, and the signal is damped out by the free induction decay.[10] When the ensemble becomes incoherent the fractional population of the excited state (which must be less than the ratio of photons to quantum well electrons) is less than 10^{-6}. These carriers relax during the time between pulses (12.5 ns). Therefore our measurements only probe the linear optical properties of the QWs.

We now show how the linear optical properties of the sample can be extracted from the cross-correlation signal. The power falling on the integrating detector is given by

$$S(t_0) = \int_{-\infty}^{\infty} [E_S(t) + E_A(t+t_0)]^2 dt, \tag{1}$$

where $E_S(t)$ and $E_A(t)$ describe the electric field at the detector from the sample-beam and analysis-beam pulses, and t_0 is the delay between the pulses. The term which varies with delay is the cross-correlation signal

$$X(t_0) = \int_{-\infty}^{\infty} E_S(t) E_A(t+t_0) dt. \tag{2}$$

The (complex) frequency spectrum is the Fourier transform of the time-domain function

$$E_S(t) = \frac{1}{2\pi} \int_{-\infty}^{\infty} E_S(\omega) e^{i\omega t} d\omega \tag{3}$$

In the following, we describe the optical properties of the sample in terms of a complex transfer function $T(\omega)$ where $E_S(\omega) = T(\omega) E_0(\omega)$, and $E_0(\omega)$ is the frequency spectrum of the sample beam when the sample is removed. The sample transfer function is found to be the ratio of the cross-correlation signal and a reference signal recorded with the sample removed $X_0(t)$

$$T(\omega) = \int_{-\infty}^{\infty} X(t_0) e^{i\omega t_0}\, dt_0 \Big/ \int_{-\infty}^{\infty} X_0(t_0) e^{i\omega t_0}\, dt_0. \tag{4}$$

In Fig. 3 we display the amplitude and phase of the complex transfer function associated with the intersubband transition. The reference signal $X_0(t)$ is measured with the QW depleted. The sample signal $X_S(t)$ is the sum of the signal measured while modulating the carrier density (Fig. 2) and $X_0(t)$. As seen in Fig. 3, we can get an excellent fit to the data using a transfer function derived from a single-oscillator model of the electric susceptibility of the QW electrons. In the model, the sample is treated as a uniform effective medium and the intersubband frequency, oscillator strength, and dephasing rate of the electrons are adjusted to best fit the data. The best fit yields an intersubband frequency $\nu_{12} = 1.51$ THz (50.3 cm^{-1}), an electron oscillator strength of $f = 0.6$, and a lifetime for dephasing of the electric field

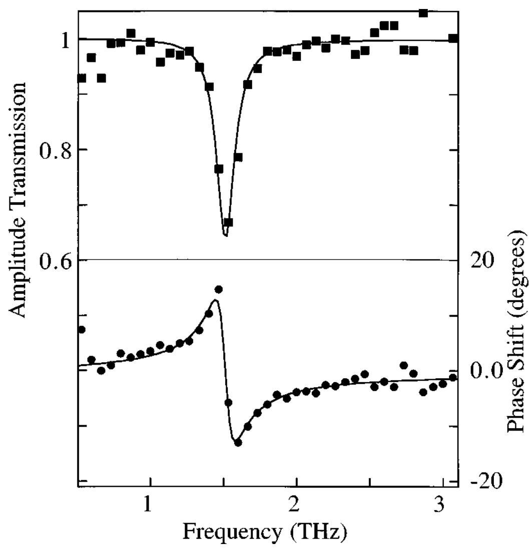

FIG. 3. Transmission coefficient for the electric field amplitude and the phase shift of the electric field due to the quantum well electrons. Dots are calculated from our cross-correlation data. Solid lines are derived from the single-oscillator model used in Fig. 2.

amplitude $\tau = 2.4$ ps. Finally, we can use this model transfer function together with the reference signal to simulate a cross-correlation signal (Fig. 2) which can be directly compared to our experimental data.

We simulated our structure by self-consistently solving the Schrodinger and Poisson equations within the effective mass approximation. The calculated intersubband absorption frequency (including the depolarization shift) fits the experimental data when the well width is set to 510 Å, which agrees with the design width (540 Å) within the margin of error. The calculated subband spacing is then $E_{12} = 5.1$ meV (41.1 cm^{-1}). Since the Fermi energy is only 1 meV, only the lowest subband in the quantum well is appreciably occupied at $T = 6$ K ($n_2/n_1 \sim 10^{-4}$). We are confident that we observe only the $n=1$ to $n=2$ transition because other transitions from $n=1$ are much weaker and occur at higher frequencies. The calculated electron oscillator strength for the $n=1$ to $n=2$ transition is $f_{1.2} = 0.93$, larger than the experimental value $f_{1.2} = 0.6$. Similar ''anomalously weak'' absorption in wide quantum wells has been observed by others,[11] and has been tentatively attributed to the breakdown of the approximation of the sample as a uniform effective medium.[12]

Our data also allow us to measure the index of refraction

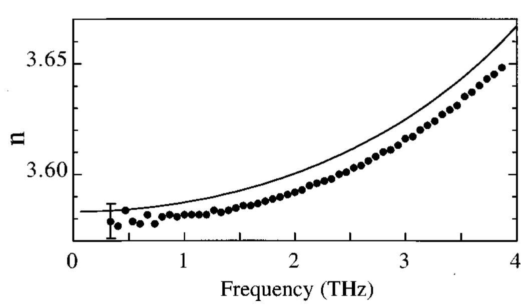

FIG. 4. Index of refraction of the depleted sample (SI-GaAs substrate) calculated from the cross-correlation data in Fig. 2. The solid line is the calculated index of refraction of bulk GaAs at low temperature. Error bar reflects uncertainty in sample length.

of the depleted sample from the phase ϕ_T of the transfer function using $n(\omega) = \phi_T(c/\omega x) + 1$, where x is the length of the sample (6.06 ± 01 mm). We have plotted in Fig. 4 the data together with the index of refraction calculated using[13]

$$\epsilon(\omega) = \epsilon(\infty)\left(\frac{\omega_L^2 - \omega^2}{\omega_T^2 - \omega^2}\right). \tag{5}$$

The index of refraction determined by our THz-TDS measurement is in excellent agreement with the calculation, which has no free parameters. This is an important check of the accuracy of our technique.

In conclusion, we have made time-domain measurements of intersubband charge oscillations in a quantum well. Our all-THz measurements quantitatively determine the linear optical constants of the sample. Our results can be understood in terms of a single oscillator model of the intersubband transition. Our measurements also give the index of refraction of the sample as a function of frequency, in excellent agreement with well known results. We have additionally studied intersubband transitions in parabolic and coupled quantum wells with THz-TDS, and we intend to report these results elsewhere.

The authors thank Ken Campman and Arthur C. Gossard of the University of California at Santa Barbara for supplying the multi-quantum well structure investigated here, and Gottfried Strasser of the F.K.E. TU-Wien for supplying the THz emitters. The authors acknowledge the support of the Austrian Science Foundation (START Y47) for this work, and J.H. acknowledges the support of an award from Research Corporation.

[1] See, for example, J. Opt. Soc. Am. **11**, 2454 (1994).
[2] H. G. Roskos, M. C. Nuss, J. Shah, K. Leo, D. A. B. Miller, A. M. Fox, S. Schnitt-Rink, and K. Köhler, Phys. Rev. Lett. **68**, 2216 (1992).
[3] P. C. M. Planken, M. C. Nuss, I. Brener, K. W. Goossen, M. S. C. Luo, S. L. Chuang, and L. Pfeiffer, Phys. Rev. Lett. **69**, 3800 (1992).
[4] C. Waschke, H. G. Roskos, R. Schwedler, K. Leo, H. Kurz, and K. Köhler, Phys. Rev. Lett. **70**, 3319 (1993).
[5] A. Bonvalet, J. Nagle, V. Berger, A. Migus, J.-L. Martin, and M. Joffre, Phys. Rev. Lett. **76**, 4392 (1996).
[6] I. Brener, P. C. M. Planken, M. C. Nuss, M. S. C. Luo, S. L. Chuang, L. Pfeffer, D. E. Leaird, and A. M. Weiner, J. Opt. Soc. Am. **11**, 2457 (1994).
[7] A. P. Heberle, J. J. Baumberg, and K. Köhler, Phys. Rev. Lett. **75**, 2598 (1995).
[8] D. Some and A. V. Nurmikko, Appl. Phys. Lett. **65**, 3377 (1994).
[9] R. Kersting, K. Unterrainer, G. Strasser, H. K. Kauffmann, and E. Gornik, Phys. Rev. Lett. **79**, 3038 (1997).
[10] We have obtained essentially identical results (but with higher noise) by analyzing the cross-correlation signals measured at 0 V bias and at -10 V bias.
[11] K. Craig, Ph.D. thesis (unpublished), University of California at Santa Barbara, 1997.
[12] M. Zaluzny, Solid State Commun. **97**, 809 (1996).
[13] The calculation used $\epsilon(\infty) = 10.9$, after C. J. Johnson, G. H. Sherman, and R. Weil, Appl. Opt. **8**, 1667 (1969); and $\nu_{\mathrm{LO}} = 296.4\ \mathrm{cm}^{-1}$ and $\nu_{\mathrm{TO}} = 273.1\ \mathrm{cm}^{-1}$ after A. Mooradian and G. B. Wright, Solid State Commun. **4**, 431 (1966).